
Figures and figure supplements

Partitioning to ordered membrane domains regulates the kinetics of secretory traffic

Ivan Castello-Serrano *et al.*

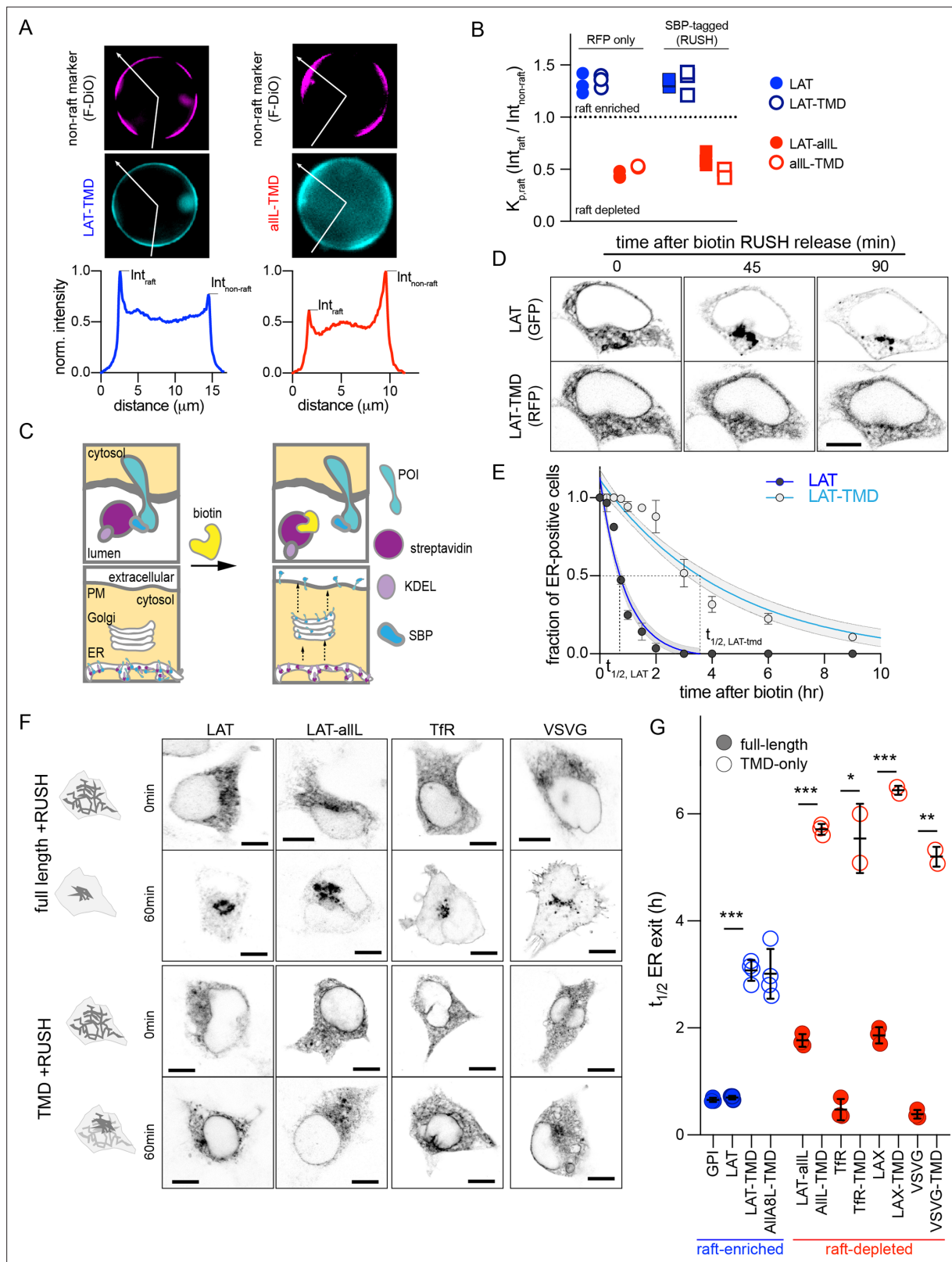


Figure 1. Full-length proteins exit the ER faster than TMD-only versions regardless of raft affinity. **(A)** Exemplary images of GPMVs from cells expressing raft-preferring LAT-TMD (left) or non-raft-preferring aILL-TMD (right). The RFP-tagged TMDs are shown in cyan; magenta shows the disordered phase marker Fast DiO (F-DiO). Bottom row shows fluorescence intensity line scans along white lines shown in cyan images, revealing protein partitioning between raft and non-raft phases. **(B)** The ratio of intensities in raft versus non-raft phase is the raft partition coefficient ($K_{p,raft}$). LAT-TMD and full-length

Figure 1 continued on next page

Figure 1 continued

LAT are enriched in the raft phase while allL-TMD (and full-length LAT with allL-TMD, LAT-allL) are largely depleted from raft phase. SBP-tagging (for RUSH assay) has no effect on raft affinity. Symbols represent 3 independent experiments with >10 GPMVs/experiment. All blue labeled constructs are not statistically different from one another, and each is $P < 0.01$ different from all red constructs. **(C)** Schematic of RUSH assay. **(D)** Confocal images of co-transfected LAT-EGFP and LAT-TMD-mRFP at various time points after biotin introduction. Full-length LAT exits ER faster. **(E)** Fraction of ER-positive cells decreases over time, allowing quantitative estimation of ER exit kinetics ($t_{1/2}$). Symbols represent average \pm st.dev. from >3 independent experiments. Fits represent exponential decays with shading representing 95% confidence intervals. **(F)** Confocal images of various full-length and TMD-only RUSH constructs (RFP-tagged) at 0 and 60 min after biotin introduction. **(G)** Quantification of $t_{1/2}$ for ER exit comparing full-length and TMD-only proteins (blue represents raft-enriched proteins, red = raft-depleted; see **Supplementary file 1** for $K_{p,raft}$ quantifications). Bars represent average \pm st.dev. from three independent experiments; * $p < 0.05$, ** $p < 0.01$, *** $p < 0.001$. All scale bars correspond to 5 μ m. Original data quantification can be found in the Source Data files.

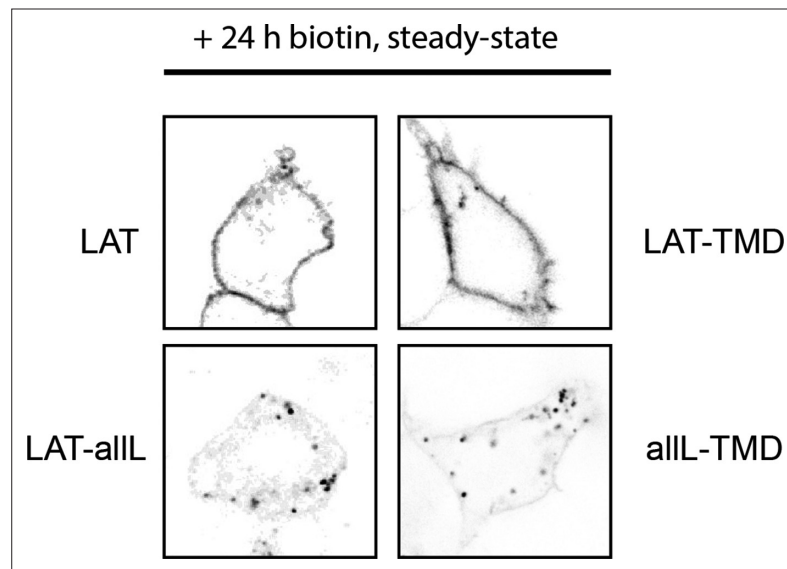


Figure 1—figure supplement 1. Representative images of RUSH constructs after overnight (>10 hr) treatment with biotin. Images show the steady-state distribution: LAT and LAT-TMD accumulate at the PM, LAT-aILL and aILL-TMD accumulate in punctate structures previously identified as lysosomes.

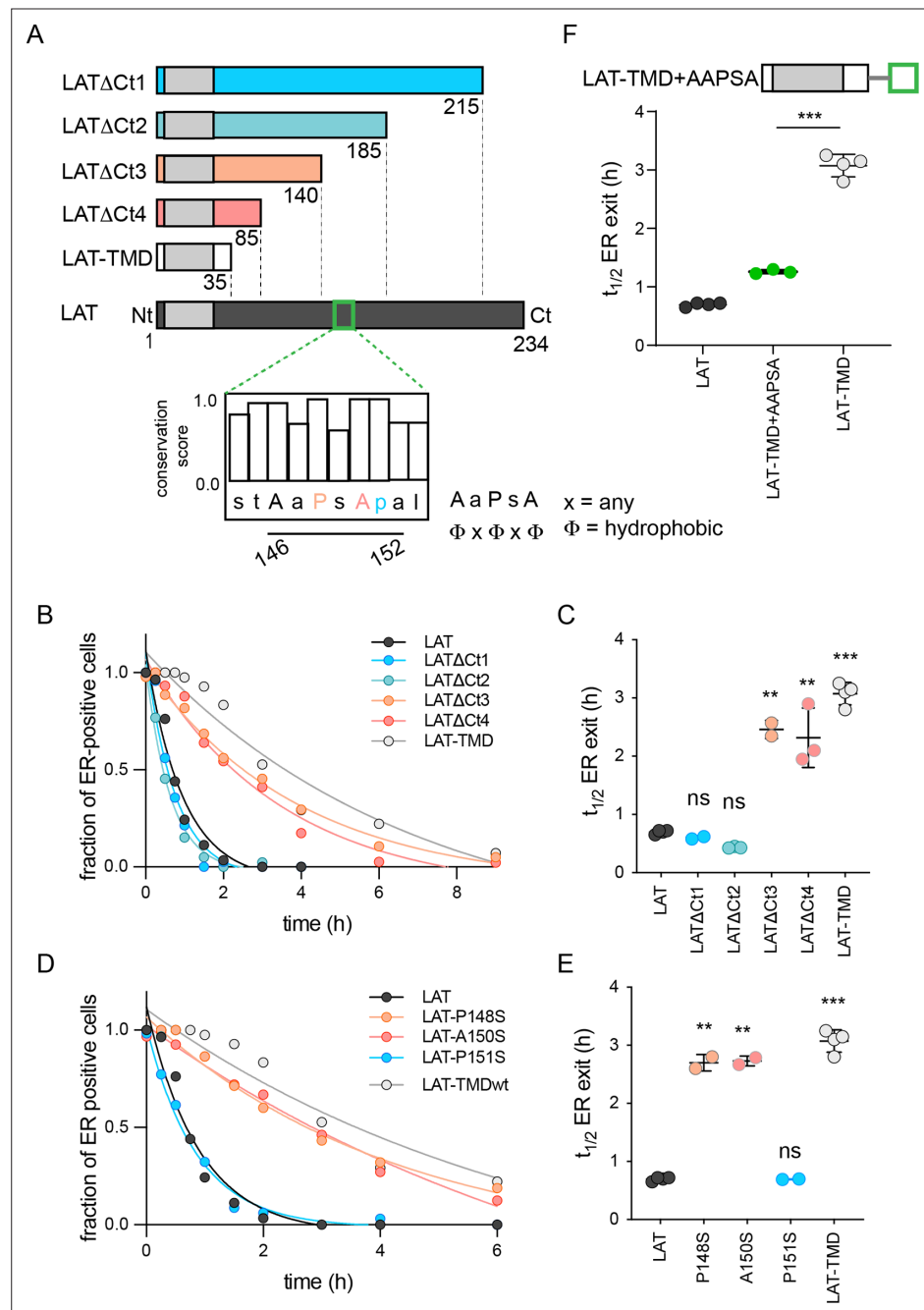


Figure 2. Identification of ER exit motif of LAT. **(A)** Schematic of LAT and the truncated versions used here. Inset shows a putative COPII association motif and the evolutionary conservation of residues 144–153 of hLAT. **(B)** Temporal dependence of the fraction of ER-positive cells for LAT truncations. Deletion of a region comprised of residues 140–185 leads to slow ER exit. **(C)** Fitted ER exit kinetics for the constructs represented in panel **C**. Deletion of amino acids 140–185 slows ER exit kinetics by ~fourfold. **(D)** Temporal dependence of fraction of ER-positive cells with point mutations of $\Phi x\Phi x\Phi$ motif. Mutations of key residues within the motif slow ER exit kinetics. **(E)** Fitted ER exit kinetics for point mutants in panel **D**. **(F)** Insertion of AaPSA motif into LAT-TMD accelerates ER exit kinetics. **(B and D)** show a representative experiment with exponential decay fits; points in **C, E, and F** represent $t_{1/2}$ values of ER exit from fits of independent repeats with >20 cells/experiment. ** $p < 0.01$, *** $p < 0.001$, nsp > 0.05. Original data quantification can be found in the Source Data files.

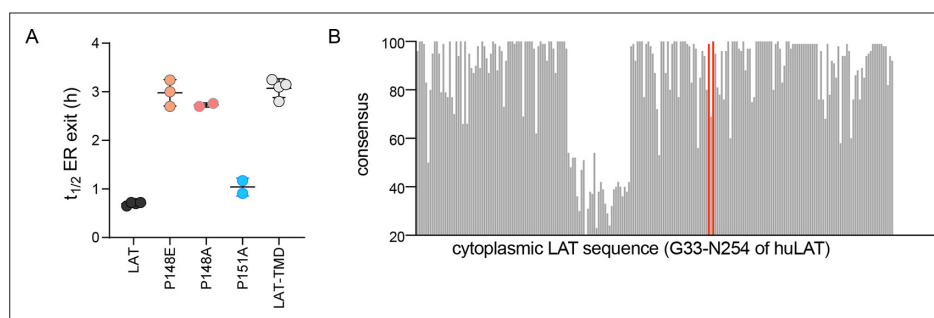


Figure 2—figure supplement 1. COPII binding motif mediates fast ER exit of LAT. **(A)** Half-time for ER exit for point mutations in the FxFxF motif of LAT. P148 is critical for fast export from the ER, P151 is not. **(B)** Evolutionary conservation of cytoplasmic residues of LAT (denoted for residues G33 through the C-terminal N254 of human LAT). Red marks P148 and A150 for comparison.

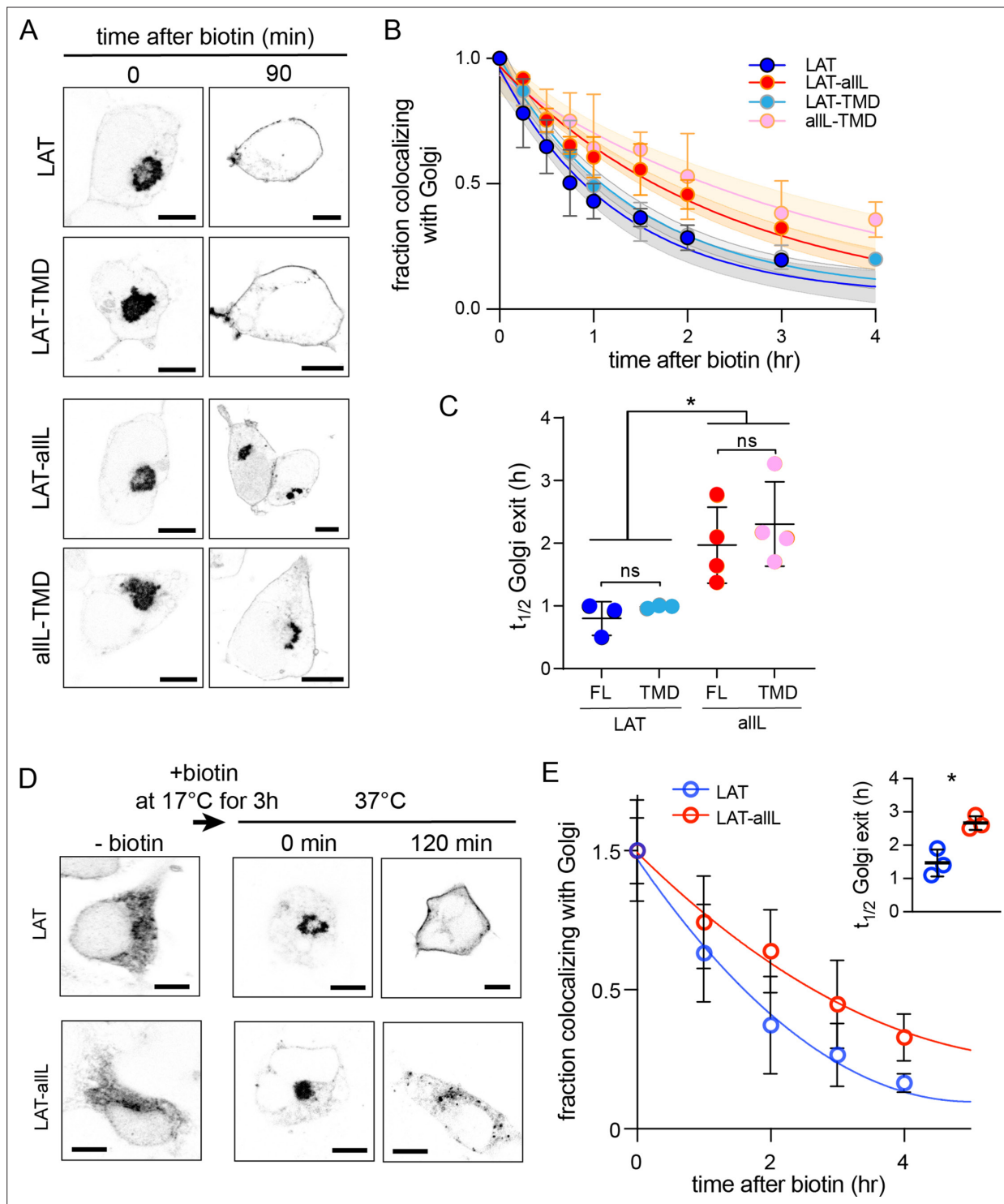


Figure 3. Golgi exit kinetics of LAT are dependent on its association with raft domains. **(A)** Representative confocal images of Golgi RUSH experiment show notable Golgi retention of non-raft constructs (LAT-aLL and aLL-TMD) after 90 min of biotin addition, in contrast to raft-preferring LAT and LAT-TMD. **(B)** Temporal reduction of protein constructs remaining in Golgi after biotin addition (i.e. release from Golgi RUSH), quantified by immunostaining and colocalization with Golgi marker (Giantin, see **Figure 3—figure supplement 2**). Symbols represent average \pm st.dev. from three independent experiments with >15 cells/experiment. Fits represent exponential decays; shading represents 95% confidence intervals. **(C)** Golgi exit rates for raft-associated LAT constructs are ~ 2.5 -fold faster than non-raft versions for both full-length and TMD-only. Points represent $t_{1/2}$ values from fits of independent repeats with >20 cells/experiment. $*p < 0.05$, $^{ns}p > 0.05$. **(D)** Representative confocal images of full-length LAT and LAT-aLL during Golgi temperature block. Addition of biotin at 17 °C releases ER-RUSH constructs but traps them in Golgi. Removing temperature block by incubation at

Figure 3 continued on next page

Figure 3 continued

37 °C leads to fast PM trafficking of LAT but not non-raft LAT-allL. **(E)** Fraction of proteins in Golgi for the constructs shown in D, calculated as in B. Fits represent exponential decays. (inset) Golgi exit kinetics quantified as in C. All scale bars = 5 μ m. Original data quantification can be found in the Source Data files.

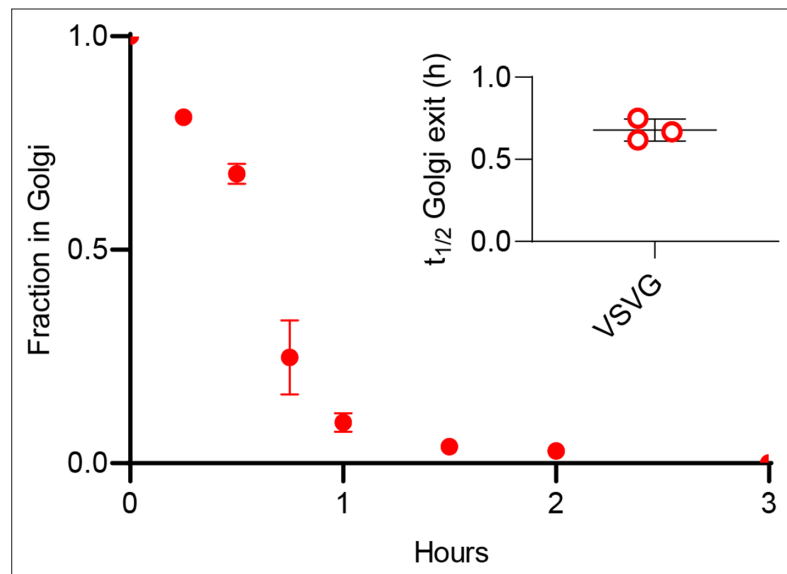


Figure 3—figure supplement 1. Fraction of RUSH-VSVG in Golgi after biotin addition. Inset represents repeats quantifications of the half-time of Golgi exit. Symbols represent average \pm st.dev. from three independent experiments.

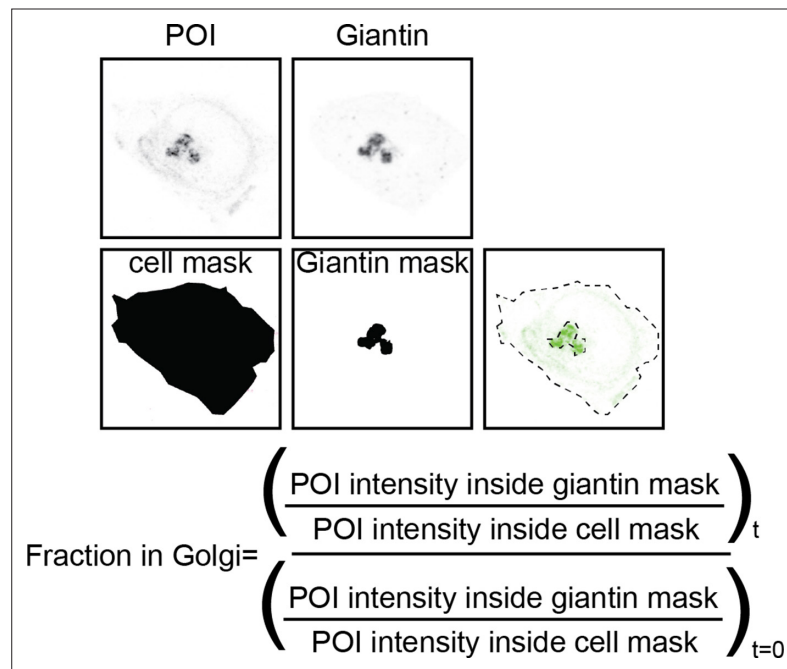


Figure 3—figure supplement 2. Example of quantification of Golgi residence for protein of interest (POI). Top panels are representative images, bottom panels are corresponding masks to calculate the fraction of POI in Golgi. Giantin was used as Golgi marker to create the mask for that organelle. Cells mask represents the cell border from the POI channel after background subtraction.

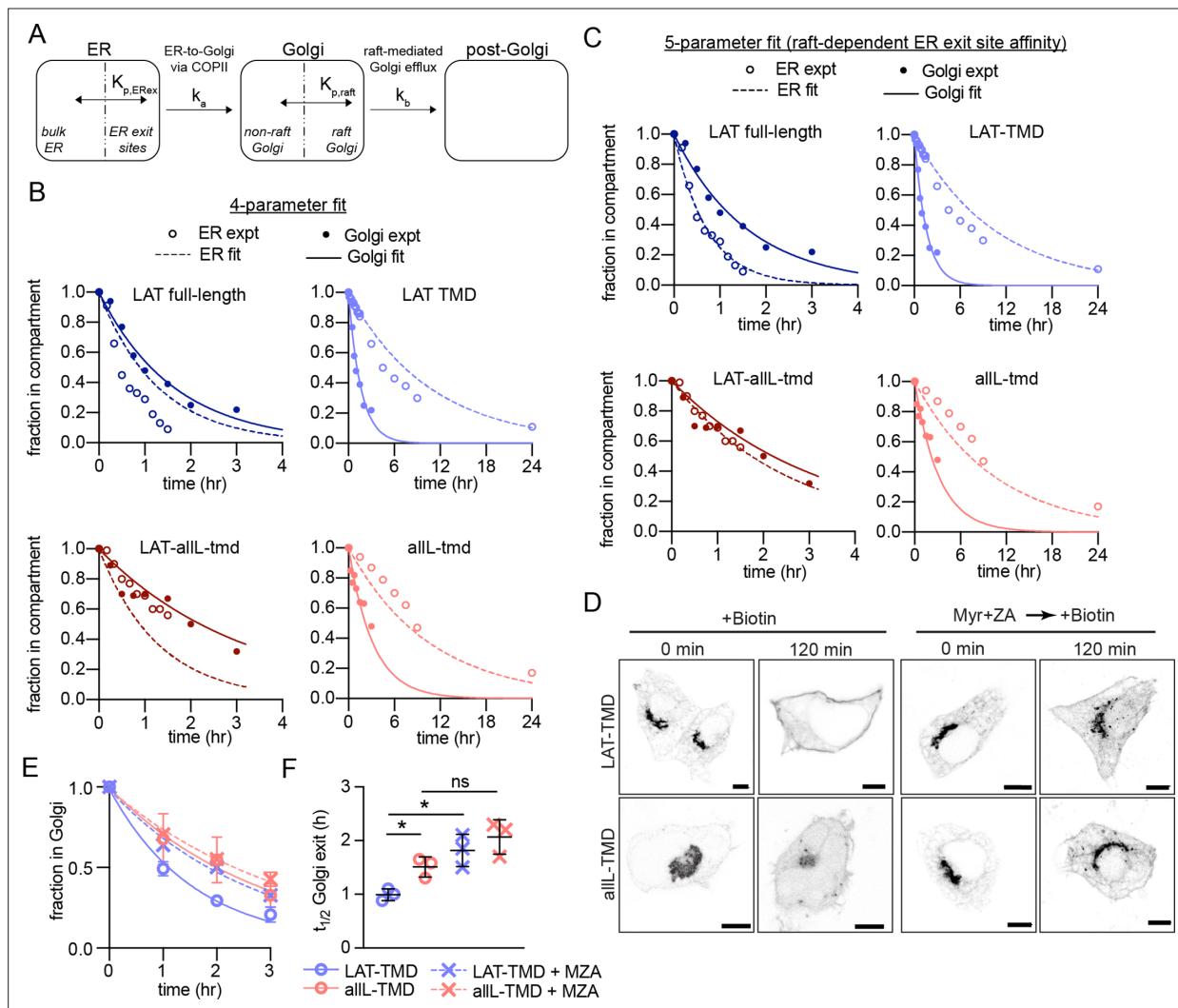


Figure 4. Kinetic model describing secretory traffic of LAT-based constructs. **(A)** Schematic of kinetic model. **(B)** Global fit of model with four free parameters to ER and Golgi RUSH data for four experimental constructs. **(C)** Global fit of model with five free parameters (different $K_{p,ERex}$ for LAT and LAT-allL). **(D)** Representative confocal images of Golgi RUSH experiments show notable Golgi retention for raft-prefering LAT after 2 day pre-treatment with Myr +ZA. Scale bars = 5 μ m. **(E)** Temporal dependence of the fraction of protein constructs remaining in Golgi after biotin addition (to release from Golgi RUSH). Symbols represent average \pm st dev from three independent experiments with >15 cells/exp. **(F)** Golgi exit rate for the raft-probe LAT-TMD is reduced when raft lipid synthesis is inhibited by Myr-ZA treatment. Points represent $t_{1/2}$ values of Golgi exit from fits of independent repeats with >20 cells/experiment. $**p < 0.01$, $^{ns}p > 0.05$. Original data quantification can be found in the Source Data files.

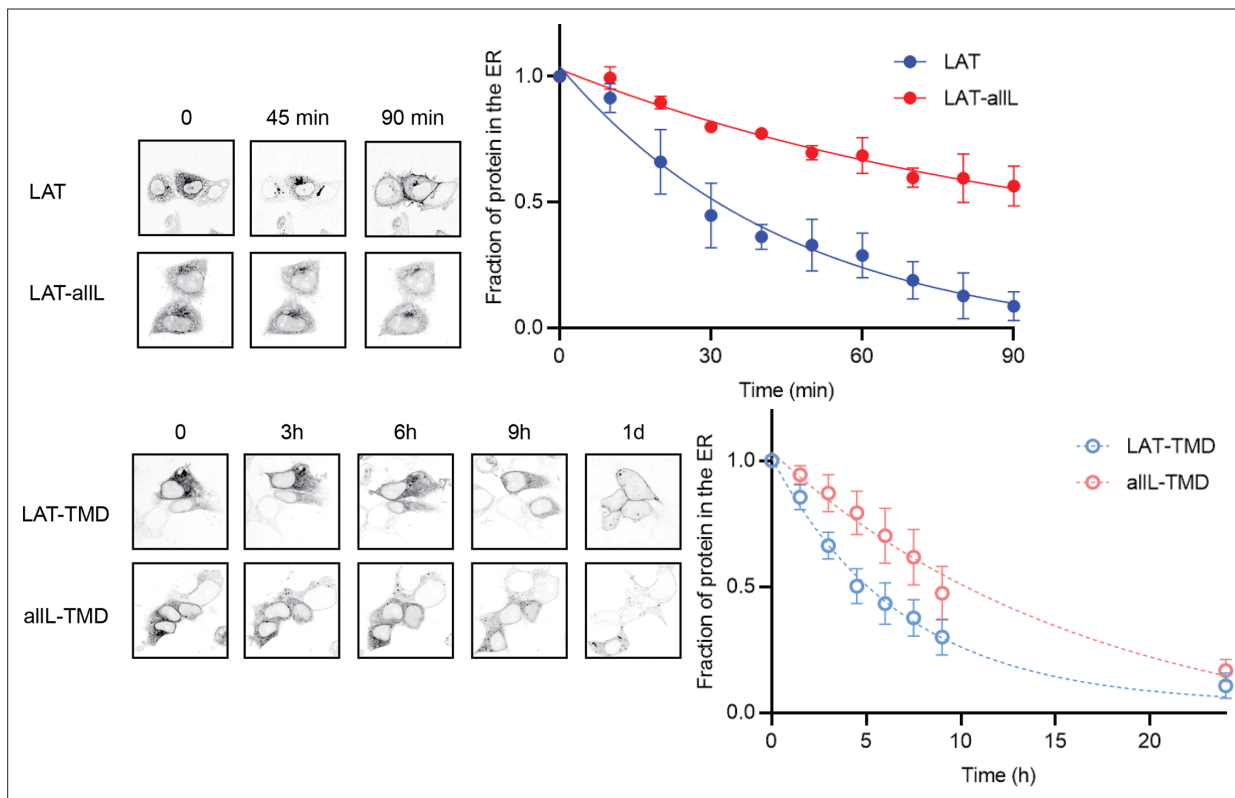


Figure 4—figure supplement 1. Representative images of the experiments measuring ER exit kinetics within individual cells, used for the kinetic modeling. Images show localization of RUSH constructs within a set of cells after biotin addition. Fraction in ER was quantified by making a mask of the protein at time 0 (i.e. before biotin addition) and calculating the remaining intensity within the mask (relative to total cellular intensity) at each subsequent time point. Top panels show full-length LAT and LAT-aIIIL, bottom panels are LAT-TMD and aIIIL-TMD. Symbols represent average \pm st.dev. from three independent experiments with multiple cells per experiment.

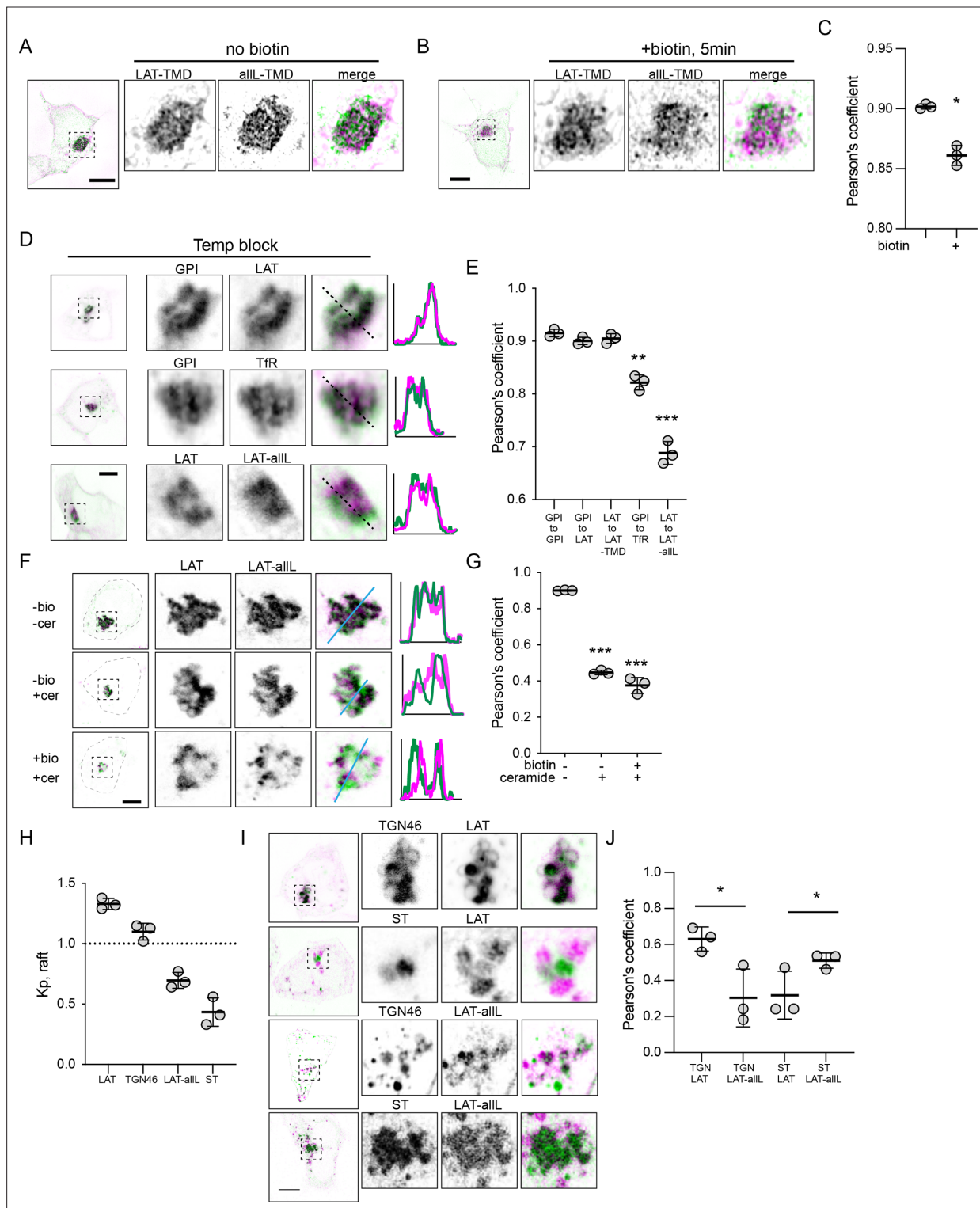


Figure 5. Raft probes segregate from non-raft in Golgi. **(A)** Raft vs non-raft probes trapped in Golgi by Golgi-RUSH (i.e. without biotin) and imaged by structured-illumination microscopy (SIM). **(B)** SIM images of localization of raft vs non-raft probes after 5 min of biotin addition to release Golgi RUSH. **(C)** Quantification of colocalization from SIM images by Pearson's coefficient in A and B. Symbols represent average \pm st. dev. from three independent experiments with >15 cells/experiment. **(D)** Confocal images of cellular localization of co-transfected probes in cells grown at 20 °C to accumulate probes in Golgi. **(E)** Quantification of colocalization under the conditions represented in D. Significances shown are relative to LAT-to-LAT-TMD. **(F)** Images of cellular localization of co-transfected Golgi-RUSH probes after treatment with biotin or C6-Cer. **(G)** Quantification of colocalization under the conditions represented in F. Significances shown are relative to -biotin/-Cer. **(H)** Quantification of raft affinity ($K_{p,raft}$) of TGN46 and ST,

Figure 5 continued on next page

Figure 5 continued

representatives of different Golgi sub-compartments. **(I)** Representative images of raft probes relative to Golgi sub-compartment markers under C6-Cer treatment. **(J)** Quantification of colocalization of proteins represented in I. Symbols in all quantifications are average \pm st. dev. from three independent experiments with >15 cells/experiment. * $p < 0.05$. Original data quantification can be found in the Source Data files.